



# CNT-sandwiched copper composites as super thermal conductors for heat management

Pengjie Wang<sup>a,b</sup>, Qiang Cao<sup>a,b,\*</sup>, Huaipeng Wang<sup>a,b</sup>, Sheng Liu<sup>a,b</sup>, Yuanping Chen<sup>c</sup>, Qing Peng<sup>d,e,\*\*</sup>

<sup>a</sup> The Institute of Technological Sciences, Wuhan University, Wuhan, 430072, China

<sup>b</sup> Key Laboratory of Hydraulic Machinery Transient, Ministry of Education, Wuhan University, China

<sup>c</sup> Faculty of Science, Jiangsu University, Zhenjiang, 212013, Jiangsu, China

<sup>d</sup> Physics Department, King Fahd University of Petroleum & Minerals, Dhahran, 31261, Saudi Arabia

<sup>e</sup> K.A.CARE Energy Research & Innovation Center at Dhahran, Dhahran, 31261, Saudi Arabia

## ARTICLE INFO

### Keywords:

CNT/Cu/CNT nanocomposite  
Lattice thermal conductivity  
Thermal transport mechanism  
Thermal stress

## ABSTRACT

Due to outstanding electric conductance, copper is widely used as wires in electricity and as interconnects in microchips, where the thermal conductivity could be enhanced by compositing with carbon nanotubes (CNTs). Here, we have numerically designed a class of sandwich-like CNT/Cu/CNT nanotubes which possess high thermal conductivity revealed by molecular dynamics simulations. The enhancement factor of thermal conductivity of the composite using single-walled CNT is 37.5 times of that of a 5-nm-radius copper nanowire. The enhancement factor is further enlarged to 58.2 using triple-walled CNT in the outer side. The atomic stress analysis manifests that the thermal stresses are concentrated in the region around the CNT/Cu interface. The stabilities and larger enhancement factors at high temperatures imply high temperature applications of these CNT-sandwiched tubular copper nanocomposites in heat management and electronics.

## 1. Introduction

Since their discovery [1], Carbon nanotubes (CNTs) exhibit unique mechanical, electronic and thermal properties, attracting considerable research efforts in energy conversion, ultra-high-strength nanocomposites, optical and electronic devices [2–5]. In the past decade, extensive attentions have been paid on the CNTs and CNT-based nanocomposites in terms of their potential applications due to their exceptional mechanical and physical characteristics, especially the composites with metal or polymer matrixes [6–10]. In particular, the CNT-reinforced metallic nanocomposites are believed to have promising applications in electronic equipment and ultra-large-scale integrated circuits on account of their potentially super electronic and thermal conductivities, providing a new way to further reduce the additional power consumptions and circuit size [8,11].

Conventionally, copper is used predominately in electrical generators, wirings, transformers and micro interconnectors, as well as industrial machinery components due to its highly heat-conductive and current-carrying capacity among metals [12]. However, with the aim

of high sustainability, reliability and efficiency of the next-generation microscale applications, looking for a lighter alternative to replace the heavy copper parts has become a central task currently. In view of this, the CNT/Cu composite is an excellent choice owing to its light weight and corrosion resistance, as well as the high electron and phonon mobilities of the CNTs [13], thus attracting a range of investigations, both theoretically and experimentally [14–17].

As electronics tend to be more integrated and slimmer, there is a growing need to design the heat and electric management precisely for higher stability, efficiency and functionality. Consequently, although many reported studies have focused on the CNT-reinforced metal-matrix nanocomposites [18–20], the questions still remain as to how to design a high-performance composite structure to take proper advantage of the outstanding mechanical properties, intrinsic thermal and electronic conductivity of CNTs. Therefore, we numerically designed a hybrid structure of the CNT/Cu nanocomposite with ultrahigh strength, superior thermal and electronic transport capacities. The heat flux and electric current mainly flow inside the CNT region.

In the present study, we report a design, atomic structure, stability,

\* Corresponding author. The Institute of Technological Sciences, Wuhan University, Wuhan, 430072, China.

\*\* Corresponding author. The Institute of Technological Sciences, Wuhan University, Wuhan, 430072, China.

E-mail addresses: [caoqiang@whu.edu.cn](mailto:caoqiang@whu.edu.cn) (Q. Cao), [qpeng.org@gmail.com](mailto:qpeng.org@gmail.com) (Q. Peng).

thermal properties, and thermal transport mechanism of the hybrid structure of the CNT/Cu/CNT tubular nanocomposite using molecular dynamic (MD) simulations. The enhancement on thermal conductive capacity was revealed by phonon density of states (PDOS). We have compared thermal properties of the nanocomposite structure with the pristine copper nanowire and isolated single-walled CNT in the same external diameter. Additionally, the effects of multilayer CNTs and ambient temperatures, as well as the thermal stress on the thermal conductivity were discussed in detail.

## 2. Method

Molecular dynamics simulation is a well-established and powerful tool to investigate materials properties [21]. We employ the classical MD simulations to model thermal conduction process of the sandwich CNT/Cu/CNT composite structure, implemented by the Large-scale Atomic/Molecular Massively Parallel Simulator (LAMMPS) [22]. We have studied the composite configuration with the outer and inner CNTs, in the radius of 5 nm and 3 nm, respectively. The isolated single-walled CNT with varied radii and pristine FCC copper with a lattice constant of 0.3615 nm were performed for comparison. Both the isolated CNT and composite cases have a length of 20 nm. The periodic boundary condition is applied to the axial (y) directions.

We adopted the adaptive intermolecular reactive empirical bond order (AIREBO) potential to describe the interactions between carbon atoms, which is widely utilized for the carbon material simulations [23, 24]. The embedded-atom method (EAM) empirical potential was used for the interactions between copper atoms [25]. We adopted the classical Lennard Jones (LJ) potential for the C–Cu interaction, owing to that there were no bonds produced between carbon and copper atoms. The parameters  $\sigma$  and  $\epsilon$  for the C–Cu interaction are 3.0 Å and 0.0117 eV for the outer CNT, 2.84 Å and 0.0351 eV for the inner CNT, respectively [26, 27].

After creation of the model, we have firstly carried out a relaxation process of 1000 ps to equilibrate the initial atomistic structures, including 500 ps of NPT canonical ensemble and 500 ps of NVE ensemble. The Nose-Hoover algorithm is employed for the temperature controlling at 300 K [28]. In the simulations of the thermal conductivities, the non-equilibrium MD simulation method is adopted with a context of NVE ensemble. The movies of the thermal conductive processes are [Movie S1, S2, S3 in Supplementary Information](#) for the sandwich-like tubular nanocomposite structure with the single-walled CNT, double-walled CNT and triple-walled CNT in the outer side, respectively, proving the stability of the sandwich-like tubular structure. A timestep of 0.0001 ps was set and 5,000,000 timesteps were conducted in all the simulations. The thermal stress analyses were performed using OVITO [29].

## 3. Results and discussion

### 3.1. Thermal transport of CNT/Cu/CNT nanocomposites

On account of the strong covalent bonds between carbon atoms, the thermal transport in carbon allotropes is mainly contributed by phonons rather than electrons [30,31], whereas it comes to the opposite completely in the copper matrix. The mechanism of thermal transport in the CNT/Cu/CNT nanocomposite is graphically displayed in [Fig. 1a](#). In the CNT region, the thermal transport is mainly attributed to the lattice vibrations which transfer the energy from hot zone to the cold zone. While inside the copper matrix, the heat transfer relies on the collisions between the free electrons and metal cations. Due to the fact that the CNT has a much better thermal conductivity than the copper matrix, the heat fluxes flow more quickly in the CNTs from the heat source to the heat sink, as shown by the red arrows. In the meantime, there are also heat exchanges between the CNTs and copper matrix. In other words, the heat generated within the copper matrix can dissipate quickly

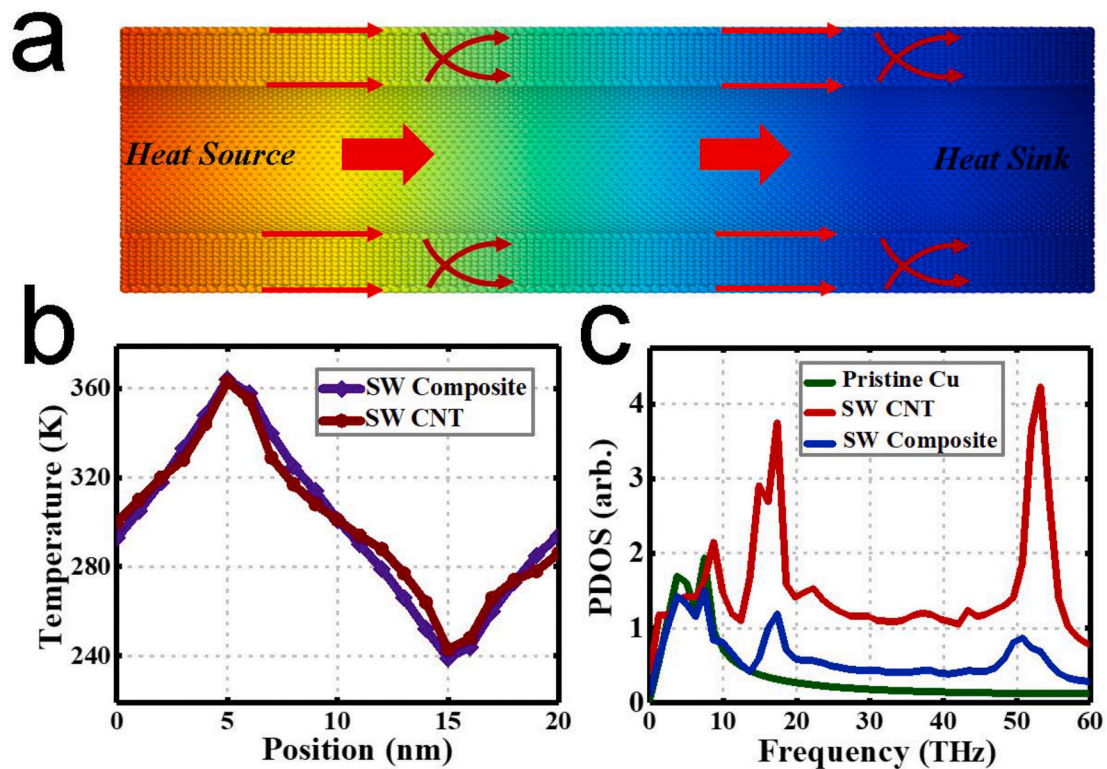


**Fig. 1.** (a) The mechanism of thermal transport in the sandwich-like CNT/Cu/CNT tubular nanocomposite structure; (b) Temperature distribution of Single-walled (SW) CNT (radius of 5 nm) and composite structure in stabilized heat-transporting situation with the same heat flux; (c) The phonon density of states (PDOS) of pristine copper nanowire, isolated single-walled CNT and the tubular nanocomposite structure at the same heat flux.

through the CNTs, which has great advantages and applications in heat management in many applications, for example, in the electronic circuits.

We have investigated the lattice thermal conductivity (LTC), which is determined primarily by phonons. The MD simulation approach is suitable because the phonon transport is dominated in the thermal conductivity of the CNT/Cu/CNT composite. We have initially carried out the thermal conductive simulations of the single-walled CNT with the radii of 1, 3, and 5 nm as reference for comparison with the studies of composites. Fig. 1b shows the stabilized temperature distribution of the single-walled CNT (radius of 5 nm) and the sandwich-like CNT/Cu/CNT tubular nanocomposite structure (inner CNT in radius of 3 nm and outer CNT in radius of 5 nm) at the same heat flux. The position 5 nm was set the heat source while the position 15 nm was a heat sink. It is demonstrated that the composite structure has a better homogeneous temperature gradient than the CNT, due to the double-layer heat-transferring effect in both the inner and outer CNTs. The lattice thermal conductivity of the single-walled CNT with a radius of 1 nm is eventually stabilized at 4407 W/m-K, consistent with the previous studies about 2000–6000 W/m-K both in experiment and theory [32,33]. The lattice thermal conductivity in the other two CNT cases is 1121 and 707 W/m-K for the radius of 3 nm and 5 nm, respectively, due to the size effect [34]. For the CNT/Cu/CNT composite structure, the lattice thermal conductivity has a fluctuates at the initial time and stabilizes around 450 W/m-K finally, which is 37.5 times that (12 W/m-K) of the lattice thermal conductivity of the 5-nm-radius pristine copper nanowire in our models.

To gain atomistic insights of the heat transport mechanism of such high thermal conductivity, we have examined the phonon density of states (PDOS). Fig. 1c shows the PDOS-frequency curves of the pristine copper nanowire, single-walled CNT and sandwich-like tubular composite structure. The PDOS of the single-walled CNT show an obviously high peak at 52 THz, which is a typical characteristic of the phonon spectrum of carbon allotropes, as well as the relatively lower peaks at 17 THz. Four types of lattice vibration exist in the CNT: a longitudinal acoustic (LA) mode related to the atom moving along the nanotube axis, two relatively low-velocity transverse acoustic (TA) modes depicting the in-plane and out-of-plane atomic motion perpendicular to the nanotube axis, and a twist mode attributed to the in-plane torsion of the carbon atoms around the axis [35]. The low-energy vibration peak at 17 THz is attributed to the TA modes (radial breathing mode) and the twist mode, corresponding to the radial and rotative vibrational displacements [36]. The frequency of the radial breathing model ( $\omega_{RBM}$ ) is determined by the diameter ( $D$ ) as  $\omega_{RBM} = \frac{c}{D} + c_2$  where  $c_1$  and  $c_2$  are experimentally determined constants, and  $D = \frac{\sqrt{3}}{\pi} d \sqrt{n^2 + nm + m^2}$  is the diameter of an (n,m) tube with  $d = 0.142$  nm the ideal C–C bond length [36].

The high frequency modes with a peak at 52 THz are mainly attributed to the vibration of the planar  $sp^2$  carbon bonds. This mode dominates the heat-transportation. According to the Boltzmann transport theory of phonons, the lattice specific heat, group velocity, and scattering of phonons influence on the lattice thermal conductivity of materials [37]. In the case of a composite, the coupling between copper matrix and CNTs breaks the reflection symmetry of the phonon modes, resulting a considerable suppression effect on the heat-transporting capacity of the LA phonons. Specifically, the two-dimensional interface between CNTs and copper matrix significantly intensifies the scattering rate and reduces the relaxation time of the phonons. In addition, the van der Waals force between CNT and copper promote the interactions between the optical phonons and acoustic phonons, reducing the group velocity of the high-frequency acoustic phonons. Meanwhile, the electron-phonon coupling and scattering can also lower the heat-transporting efficiency of the phonons. Therefore, the lattice thermal conductivity of the tubular nanocomposite structure has a dramatical reduction, compared with the isolated single-walled CNT. It is worth noting that although the interface and electron-phonon scattering are negative to the thermal conductivity, the composite structure still

possesses a much better heat-carrying ability than pristine copper, showing promising applications in advanced thermoelectrics.

### 3.2. Thermal stress analysis

Because of the mismatch of the thermal expansion in the two different components CNT and copper, the thermal stress will be produced inevitably. The thermal expansion of CNT and copper is  $21 \times 10^{-6} \text{ K}^{-1}$  and  $16 \times 10^{-6} \text{ K}^{-1}$  at room temperature, respectively [38]. In the thermal transport process, the CNTs have a higher temperature than copper matrix due to the higher thermal conductivity, shown in Fig. 2a. Therefore, the volume increment of CNTs is larger than that of copper. For the outer CNT, there will be a nano interval appeared, as shown in Fig. 2b. While in the situation of inner CNT, the thermal stress is produced at the interface. The different thermal expansions cause a compressive stress in the inner CNT and a stretchable stress in the copper matrix, shown in Fig. 2c.

Fig. 2d displays the average atom temperature as a function of the radius of the cross section. It shows that the temperature at CNT regions is highest while the middle of the copper matrix has the lowest temperature. In addition, the temperature difference between the CNT and copper matrix becomes larger from heat source to heat sink due to the different thermal diffusion rates. Fig. 2e exhibits the thermal stress distribution of the cross section by calculating the average atom stress. The interface between copper matrix and inner CNT has the higher thermal stress from heat source to heat sink due to the different thermal expansions of the two components. Furthermore, on account of the different temperature gaps, the region around outer CNT suffer from more thermal stress in the heat source, while in the heat sink, the region around the inner CNT produce the highest thermal stress.

### 3.3. Temperature effect

To explore the characteristics of the tubular nanocomposite structure at different temperatures, we carried out the studies for the single-walled composite case in varied temperatures. As displayed in Fig. 3a, the PDOS of the composite is increased with temperature in the full range of frequencies, reflecting the fact that the thermal vibrations are much severer at a higher temperature. The increased thermal vibrations enhance the phonon-electron interactions, leading to stronger phonon-electron scattering and reduced mean-free paths. As a result, the thermal conductivity decreases with respect to an increase in temperature. The detailed relationship of the thermal conductivity and temperature is illustrated in Fig. 3b. It reveals a general trend that the lattice thermal conductivity decreases with the rise of the temperature. This behavior could be understood as follows. The anharmonic phonon-phonon and electron-phonon scattering interactions called Umklapp processes are resistive to the thermal transport and closely connected to the environment temperature [39].

With the rise of the temperature, more high frequency phonons appear and participate the thermal transport process. Meanwhile, the electron-phonon and phonon-phonon interactions between copper matrix and CNTs become more intense [40]. The intensified phonon-phonon interactions enhance the phonon scattering at the interface, resulting the reduction of the thermal transport capacity [33]. It is worth emphasizing that the tubular nanocomposite structure has a relatively much higher lattice thermal conductivity, around 385 W/m-K at the high temperature of 900 K, compared to that of the 5-nm-radius pristine copper nanowire around 12 W/m-K. It is attributed to the superior conductive properties of the CNTs at high-temperature environment, giving a new expectation for the high-temperature applications.

### 3.4. Multilayer effect

The electromechanical and thermal properties have a great influence



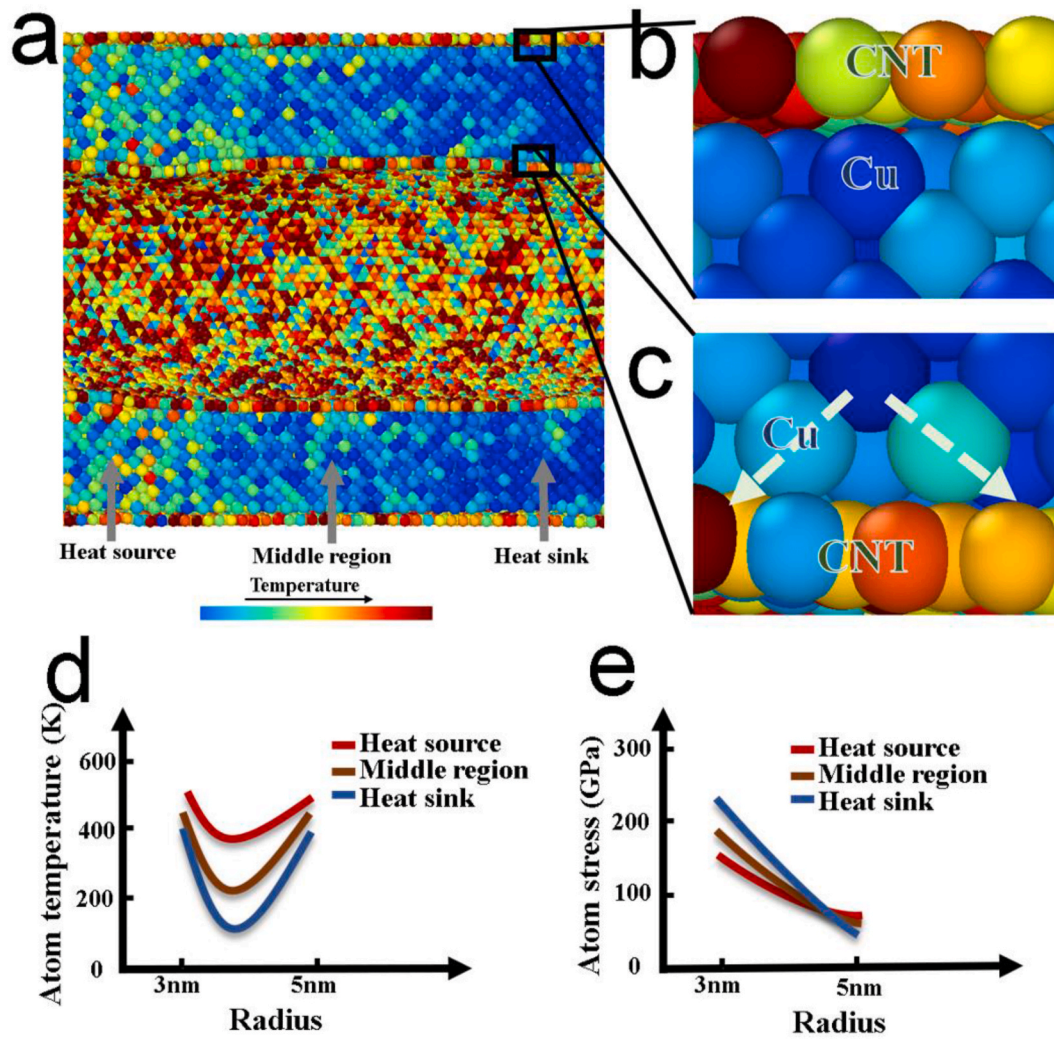


**Fig. 2.** (a) Atom-temperature distribution of the CNT/Cu/CNT nanocomposite when transporting thermal energy from heat source to heat sink; (b) The nano interval between the outer CNT and copper matrix produced during the heat-transport process; (c) Schematic diagram of the thermal stress produced between the inner CNT and copper atoms; Average (d) atom temperature and (e) atom stress change with the radius from 3 nm to 5 nm of the composite structure in the steady heat-transport process.

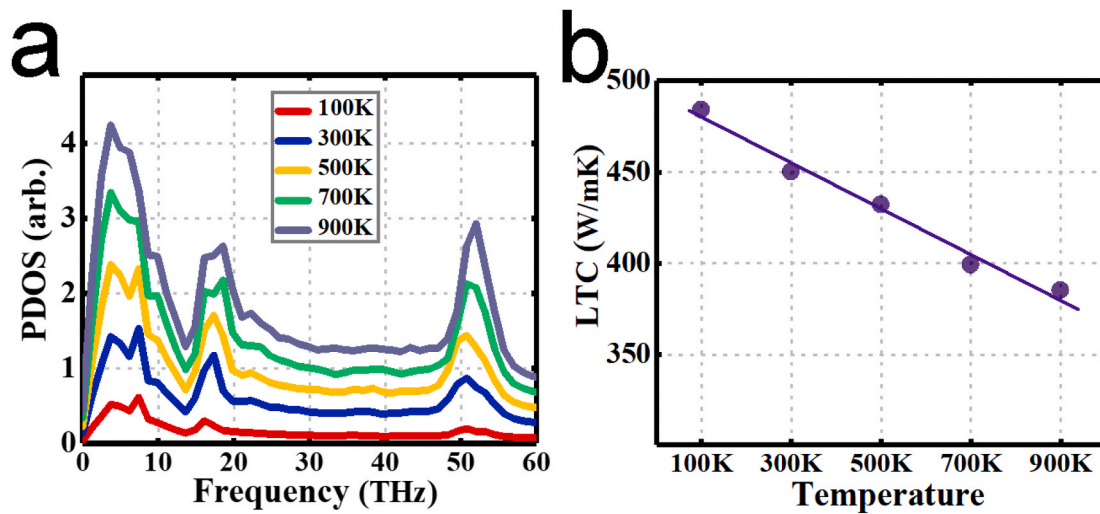


**Fig. 3.** (a) Phonon density of states (PDOS) and (b) Lattice thermal conductivities (LTC) of the sandwich-like tubular nanocomposite with single-walled CNT at varied temperatures from 100 K to 900 K.

on the applications of the multiwalled CNTs [41]. Therefore, we have explored three configurations of outer CNTs, single-walled (SW), double-walled (DW) and triple-walled (TW) CNTs. We have examined the isolated SW, DW, and TW CNTs as references for the enhancement of different layers of CNTs. The atomistic configurations of the different composite cases are displayed in Fig. 4a. Fig. 4b shows the PDOS-frequency curves of the pristine copper, composite and isolated CNT cases. The three CNT cases have nearly the same phonon spectrum on account of the same lattice structure. This could be understood as follows. For low frequency vibrations, the radius breath mode frequencies are proportional to the inverse of diameters, where the differences are negligible between the CNTs of the three configurations. The  $sp^2$  bonds determine the high frequency vibrations which has no differences between the three cases.

As the outer CNTs from monolayer to trilayer, the phonon density of the hybrid composite structure is enhanced, especially for the frequency higher than 10 THz. With the increase of the CNT layer, more substrate interactions occur between CNT and copper matrix while more phonons participate in the heat-transporting process both out-of-plane and in-plane, which strengthens the thermal transport capacity of the composite structure.

The lattice specific heat of CNT is much larger than that of copper. Thus, the lattice specific heat of the composite structure is higher than copper nanowire and increased with CNT layers. Although the phonon interactions and scatterings between different CNT layers can suppress the heat transport, the CNT/Cu/CNT nanotube composite has a higher thermal conductivity with more CNT layers after a combine of several factors above. Compared to the 5-nm-radius pristine copper, the enhancement factor increases from 37.5 to 58.2 with the CNTs from single-wall to triple-wall, as shown in Fig. 4c. Table 1 summarizes the thermal conductivities of pristine copper, single-walled CNTs with varied radii and composite cases with varied CNT layers. In our models, the tubular composite structure with triple-walled CNTs obtains the highest enhancement with a lattice thermal conductivity of 698 W/m-K, approximately 58 times of the 5-nm-radius pristine copper. In contrast

to the optimized graphene fiber (200–1290 W/m-K) reported by Xin et al. [42], the sandwich-like CNT/Cu/CNT tubular nanocomposite structure has great advantage on low-cost, stability and easy-fabrication.

It should be noted that we have considered only lattice thermal conductivity in this study and ignored the contribution from electrons due to the limitations of our MD model. Our results are valuable because the phonon transport is prominent in the thermal conductivity of the sandwich-like CNT/Cu/CNT tubular nanocomposite structure due to the strong  $sp^2$  covalent carbon bonds. It might be debatable about the precisions of each individual data, the trend of the change of the thermal conductivity due to the temperature and multilayer effects are clearly manifested. In addition, the atomistic stress study and PDOS analysis are unique insightful.

Our simulation results demonstrate the superior thermal properties of the sandwich-like tubular structure of the CNT/Cu/CNT nanocomposite. The stability and high thermal conductivity suggest broad applications in a diverse of electronic industries which need a highly effective thermal management, for instance, light-weight, high-capacity microelectronics, high-strength, low-resistance micro interactions in large-scale integrated circuits, or high-conductive, high-reliability components in aerospace system [43].

#### 4. Conclusions

We have numerically designed a class of sandwich-like CNT/Cu/CNT tubular nanocomposite. Via molecular dynamics simulations, we have identified that this kind of nanocomposites possess high thermal conductivity, which is over 37.5 times that of 5-nm-radius copper nanowires. The effect of single-walled, double-walled, and triple-walled CNTs on the thermal conductivity are examined in addition to the thermal transport mechanism. We predicted the superior thermal conductivity of the composite due to the dominated role of the CNTs in this sandwich-like tubular nanocomposite structure. Based on the phonon density-of-state analysis, we studied the thermally reinforced mechanism of the sandwich-like CNT/Cu/CNT tubular nanocomposite. It was

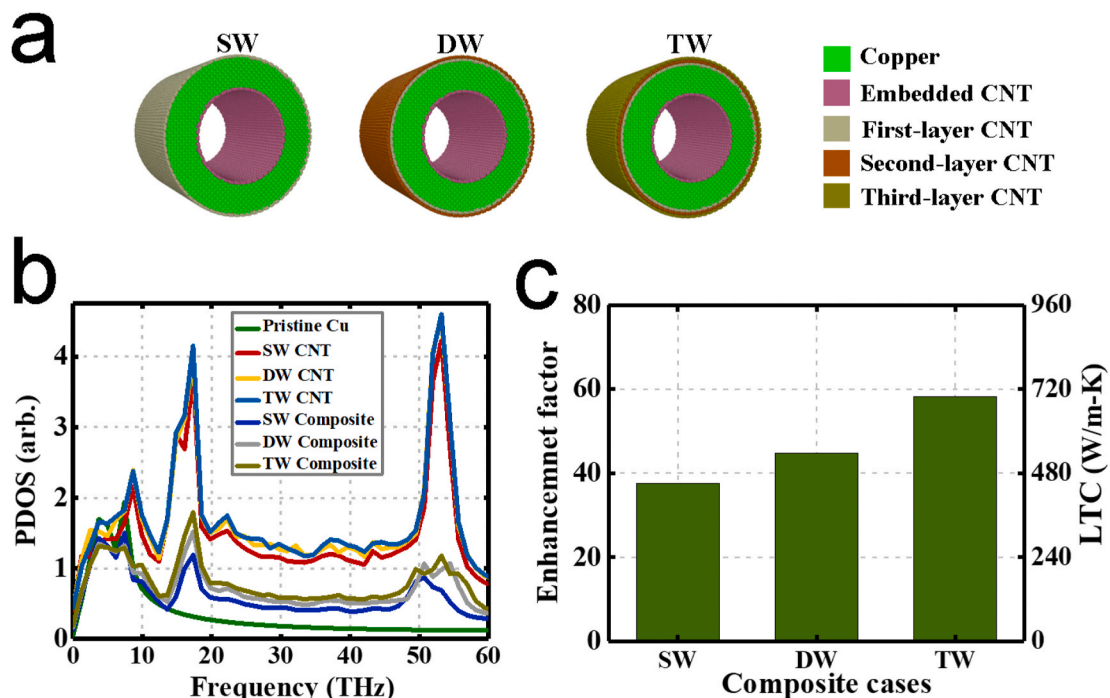


**Fig. 4.** (a) Atomic configurations of the sandwich-like CNT/Cu/CNT tubular nanocomposite cases with varied outer CNT layers; (b) Phonon density of states of pristine copper nanowire, isolated single-walled and triple-walled CNTs, and the sandwich-like CNT/Cu/CNT tubular nanocomposite cases with varied outer CNT layers at 300 K; (c) The enhancement factor and lattice thermal conductivity of the tubular nanocomposite structure cases with varied outer CNT layers at 300 K.

**Table 1**

Thermal conductivities of pristine copper, single-walled CNTs with varied radii and sandwich-like CNT/Cu/CNT tubular nanocomposite cases with varied outer CNT layers.

Composite cases	Copper nanowire (5 nm)	SW CNT (1 nm)	SW CNT (3 nm)	SW CNT (5 nm)	SW Composite	DW Composite	TW Composite
Lattice Thermal Conductivity (W/m-K)	12	4407	1121	707	450	536	698

found that the reinforcement increased with the outer CNT layers. During the thermal transport process, the thermal stress will be concentrated at the interface between CNT and copper matrix due to the temperature difference. The tubular nanocomposite structure exhibits high lattice thermal conductivity of 385 W/m-K at the environmental temperature over 900 K. The stability and excellent properties might motivate the fabrication of the CNT-sandwiched tubular copper nanocomposites. The super thermal conductivities in low and high temperatures suggest broad applications in heat management and micro- and nano-scale electronics.

### Author contributions

P-W., Q.C. and Q. P conceived the idea and wrote the paper. P.W. and H.W. did the simulations. P.W., Y.C. and S.L. performed the data analysis. All the authors had full discussions and comments on the paper.

### Data availability

All data generated or analyzed during this study are included in this published article and its supplementary information files.

### Declaration of competing interest

The authors declare no conflict of interest.

### Acknowledgments

Q.C. acknowledge the generous financial support from the Chinese Academy of Sciences under Grant (No. XDA25040201), the Fundamental Research Funds for the Central Universities under Grant (No. 2042019kf0011), and the National Natural Science Foundation of China (No. 51727901). Q. P. would like to acknowledge the support provided by the Deanship of Scientific Research (DSR) at King Fahd University of Petroleum & Minerals (KFUPM) for funding this work through project No. SR191013. The numerical calculations in this paper were conducted on the supercomputing system at the Supercomputing Center of Wuhan University.

### Appendix A. Supplementary data

Supplementary data to this article can be found online at <https://doi.org/10.1016/j.physe.2020.114557>.

### References

- [1] S. Iijima, Helical microtubules of graphitic carbon, *Nature* 354 (1991) 56–58.
- [2] R.H. Baughman, A.A. Zakhidov, W.A. de Heer, Carbon nanotubes - the route toward applications, *Science* 297 (2002) 787–792.
- [3] M.F.L. De Volder, S.H. Tawfik, R.H. Baughman, A.J. Hart, Carbon nanotubes: present and future commercial applications, *Science* 339 (2013) 535–539.
- [4] M.M. Shulaker, G. Hills, N. Patil, H. Wei, H.Y. Chen, H.S. PhilipWong, S. Mitra, Carbon nanotube computer, *Nature* 501 (2013) 526–530.
- [5] P. Avouris, Z.H. Chen, V. Perebeinos, Carbon-based electronics, *Nat. Nanotechnol.* 2 (2007) 605–615.
- [6] D.M. Sun, M.Y. Timmermans, Y. Tian, A.G. Nasibulin, E.I. Kauppinen, S. Kishimoto, T. Mizutani, Y. Ohno, Flexible high-performance carbon nanotube integrated circuits, *Nat. Nanotechnol.* 6 (2011) 156–161.
- [7] V.P. Veedu, A.Y. Cao, X.S. Li, K.G. Ma, C. Soldano, S. Kar, P.M. Ajayan, M. N. Ghasemi-Nejhad, Multifunctional composites using reinforced laminae with carbon-nanotube forests, *Nat. Mater.* 5 (2006) 457–462.
- [8] S.R. Bakshi, D. Lahiri, A. Agarwal, Carbon nanotube reinforced metal matrix composites - a review, *Int. Mater. Rev.* 55 (2010) 41–64.
- [9] I.A. Kinloch, J. Suhr, J. Lou, R.J. Young, P.M. Ajayan, Composites with carbon nanotubes and graphene: an outlook, *Science* 362 (2018) 547–553.
- [10] J.N. Coleman, U. Khan, Y.K. Gun'ko, Mechanical reinforcement of polymers using carbon nanotubes, *Adv. Mater.* 18 (2006) 689–706.
- [11] C. Subramaniam, T. Yamada, K. Kobashi, A. Sekiguchi, D.N. Futaba, M. Yumura, K. Hata, One hundred fold increase in current carrying capacity in a carbon nanotube-copper composite, *Nat. Commun.* 4 (2013) 2202.
- [12] L. Lu, Y.F. Shen, X.H. Chen, L.H. Qian, K. Lu, Ultrahigh strength and high electrical conductivity in copper, *Science* 304 (2004) 422–426.
- [13] C.H. Yu, L. Shi, Z. Yao, D.Y. Li, A. Majumdar, Thermal conductance and thermopower of an individual single-wall carbon nanotube, *Nano Lett.* 5 (2005) 1842–1846.
- [14] G. Xu, J.N. Zhao, S. Li, X.H. Zhang, Z.Z. Yong, Q.W. Li, Continuous electrodeposition for lightweight, highly conducting and strong carbon nanotube-copper composite fibers, *Nanoscale* 3 (2011) 4215–4219.
- [15] D. Janas, B. Liszka, Copper matrix nanocomposites based on carbon nanotubes or graphene, *Mat. Chem. Front.* 2 (2018) 22–35.
- [16] K.Z. Milowska, M. Burda, L. Wolanicka, P.D. Bristowe, K.K.K. Koziol, Carbon nanotube functionalization as a route to enhancing the electrical and mechanical properties of Cu- CNT composites, *Nanoscale* 11 (2019) 145–157.
- [17] C. Guiderdoni, C. Estournes, A. Peigney, A. Weibel, V. Turq, C. Laurent, The preparation of double-walled carbon nanotube/Cu composites by spark plasma sintering, and their hardness and friction properties, *Carbon* 49 (2011) 4535–4543.
- [18] S.I. Cha, K.T. Kim, S.N. Arshad, C.B. Mo, S.H. Hong, Extraordinary strengthening effect of carbon nanotubes in metal-matrix nanocomposites processed by molecular-level mixing, *Adv. Mater.* 17 (2005) 1377–1381.
- [19] G.D. Zhan, J.D. Kuntz, J.L. Wan, A.K. Mukherjee, Single-wall carbon nanotubes as attractive toughening agents in alumina-based nanocomposites, *Nat. Mater.* 2 (2003) 38–42.
- [20] A.D. Moghadam, E. Omrani, P.L. Menezes, P.K. Rohatgi, Mechanical and tribological properties of self-lubricating metal matrix nanocomposites reinforced by carbon nanotubes (CNTs) and graphene - a review, *Compos. B Eng.* 77 (2015) 402–420.
- [21] Q. Peng, F.J. Meng, Y.Z. Yang, C.Y. Lu, H.Q. Deng, L.M. Wang, S. De, F. Gao, Shockwave generates < 100 > dislocation loops in bcc iron, *Nat. Commun.* 9 (2018) 4880.
- [22] S. Plimpton, Fast Parallel algorithms for short-range molecular-dynamics, *J. Comput. Phys.* 117 (1995) 1–19.
- [23] B.H. Deng, J. Hou, H.X. Zhu, S. Liu, E. Liu, Y.F. Shi, Q. Peng, The normal-auxeticity mechanical phase transition in graphene, *2D Mater.* 4 (2017), 021020.
- [24] J. Hou, B.H. Deng, H.X. Zhu, Y.C. Lan, Y.F. Shi, S. De, L. Liu, P. Chakraborty, F. Gao, Q. Peng, Magic auxeticity angle of graphene, *Carbon* 149 (2019) 350–354.
- [25] X.W. Zhou, H.N.G. Wadley, R.A. Johnson, D.J. Larson, N. Tabat, A. Cerezo, A. K. Petford-Long, G.D.W. Smith, P.H. Clifton, R.L. Martens, T.F. Kelly, Atomic scale structure of sputtered metal multilayers, *Acta Mater.* 49 (2001) 4005–4015.
- [26] P. Wang, Q. Cao, H. Wang, Y. Nie, S. Liu, Q. Peng, Fivefold enhancement of yield and toughness of copper nanowires via coating carbon nanotubes, *Nanotechnology* 31 (2019) 115703.
- [27] B. Faria, C. Guarda, N. Silvestre, J.N.C. Lopes, D. Galhofo, Strength and failure mechanisms of cnt-reinforced copper nanocomposite, *Compos. B Eng.* 145 (2018) 108–120.
- [28] W.G. Hoover, Canonical dynamics - equilibrium phase-space distributions, *Phys. Rev.* 31 (1985) 1695–1697.
- [29] A. Stukowski, Visualization and analysis of atomistic simulation data with OVITO-the Open Visualization Tool, *Model. Simul. Mater. Sc.* 18 (2010) 15012.
- [30] L.M. Veca, M.J. Meziani, W. Wang, X. Wang, F.S. Lu, P.Y. Zhang, Y. Lin, R. Fee, J. W. Connell, Y.P. Sun, Carbon nanosheets for polymeric nanocomposites with high thermal conductivity, *Adv. Mater.* 21 (2009) 2088–2092.
- [31] J.H. Seol, I. Jo, A.L. Moore, L. Lindsay, Z.H. Aitken, M.T. Pettes, X.S. Li, Z. Yao, R. Huang, D. Broido, N. Mingo, R.S. Ruoff, L. Shi, Two-dimensional phonon transport in supported graphene, *Science* 328 (2010) 213–216.
- [32] M. Fujii, X. Zhang, H.Q. Xie, H. Ago, K. Takahashi, T. Ikuta, H. Abe, T. Shimizu, Measuring the thermal conductivity of a single carbon nanotube, *Phys. Rev. Lett.* 95 (2005), 065502.
- [33] Z.D. Han, A. Fina, Thermal conductivity of carbon nanotubes and their polymer nanocomposites: a review, *Prog. Polym. Sci.* 36 (2011) 914–944.
- [34] J.W. Che, T. Cagin, W.A. Goddard, Thermal conductivity of carbon nanotubes, *Nanotechnology* 11 (2000) 65–69.
- [35] J. Hone, Phonons and thermal properties of carbon nanotubes, *Top. Appl. Phys.* 80 (2001) 273–286.
- [36] A.J. Pool, S.K. Jain, G.T. Barkema, Structural characterization of carbon nanotubes via the vibrational density of states, *Carbon* 118 (2017) 58–65.
- [37] Z.W. Chen, X.Y. Zhang, Y.Z. Pei, Manipulation of phonon transport in thermoelectrics, *Adv. Mater.* 30 (2018) 1705617.

- [38] L.B. Deng, R.J. Young, I.A. Kinloch, R. Sun, G.P. Zhang, L. Noe, M. Monthieux, Coefficient of thermal expansion of carbon nanotubes measured by Raman spectroscopy, *Appl. Phys. Lett.* 104 (2014), 051907.
- [39] J.X. Cao, X.H. Yan, Y. Xiao, J.W. Ding, Thermal conductivity of zigzag single-walled carbon nanotubes: role of the umklapp process, *Phys. Rev. B* 69 (2004) 73407.
- [40] Z.W. Zhang, Y.E. Xie, Q. Peng, Y.P. Chen, Thermal transport in MoS<sub>2</sub>/Graphene hybrid nanosheets, *Nanotechnology* 26 (2015) 375402.
- [41] P. Kim, L. Shi, A. Majumdar, P.L. McEuen, Thermal transport measurements of individual multiwalled nanotubes, *Phys. Rev. Lett.* 87 (2001) 215502.
- [42] G.Q. Xin, T.K. Yao, H.T. Sun, S.M. Scott, D.L. Shao, G.K. Wang, J. Lian, Highly thermally conductive and mechanically strong graphene fibers, *Science* 349 (2015) 1083–1087.
- [43] L.K. Randeniya, A. Bendavid, P.J. Martin, C.D. Tran, Composite yarns of multiwalled carbon nanotubes with metallic electrical conductivity, *Small* 6 (2010) 1806–1811.